

Properties of Polyetherimide/Graphite Composites Prepared Using Ultrasonic Twin-Screw Extrusion

Jing Zhong, Avraam I. Isayev

Department of Polymer Engineering, University of Akron, Akron, Ohio 44325

Correspondence to: A. I. Isayev (E-mail: aisayev@uakron.edu)

ABSTRACT: The dispersion of various graphites in polymers is a challenging problem limiting their potential use. To solve this problem, an ultrasound assisted twin-screw extruder was developed and utilized to compound polyetherimide (PEI) with untreated nature graphite (UG), modified graphite (MG) and expanded graphite (EG) at concentrations up to 10 wt %. The effect of ultrasonic amplitude on rheological, mechanical and electrical properties of the PEI composites was investigated. Ultrasonic treatment of PEI/UG composites showed little effect on these properties. In contrast, ultrasonic treatment of PEI/MG and PEI/EG composites led to an increase of the storage (G'), loss (G'') moduli and complex viscosity and to a decrease of the damping characteristics. In particular, the PEI/5 wt %EG composite ultrasonically treated at an amplitude of 10 μm showed a 45% higher complex viscosity than the untreated composite at a frequency of 0.5 rad/s. Also, the PEI/5 wt % EG composite treated at an amplitude of 10 μm showed a reduction in the electrical volume resistivity by almost three orders of magnitude leading to a lower percolation threshold. The untreated and treated PEI/UG and PEI/MG composites did not show any percolation within all graphite concentrations studied, due to large size of particles of UG and MG and their strong agglomeration. The ultrasonic treatment showed slight effect on mechanical properties of all these composites. © 2014 Wiley Periodicals, Inc. *J. Appl. Polym. Sci.* **2015**, *132*, 41397.

KEYWORDS: composites; extrusion; mechanical properties; morphology; rheology

Received 26 June 2014; accepted 19 August 2014

DOI: 10.1002/app.41397

INTRODUCTION

Graphite which is abundant in the earth was studied for long time. The discovery of fullerenes in 1985¹ and carbon nanotubes (CNTs) in 1991² attracted further interests in studying the nanostructure of graphite. Graphite is a layered material with each layer in the form of graphene. The graphene becomes a more important material due to its excellent mechanical, thermal and electrical properties.³ However, the difficulty in converting graphite into graphene limits its application in nanocomposites. In order to obtain full utilization of graphite in polymer composites, it is desirable to exfoliate the layered structure and uniformly disperse it throughout the polymer matrix.⁴ So far, many modifications of graphite have been reported to get the exfoliated layers, such as graphite oxide (GO),⁵ graphite intercalated compounds (GIC),⁶ and expanded graphite (EG).⁷ The preparation of polymer/graphite-based composites is usually carried out using two methods: solution mixing and melt mixing.⁸ Although the solution mixing could achieve good dispersion, melt mixing is more preferable since it is efficient, environmentally friendly and compatible with the current industrial practice.⁹ The melt mixing method has been used to prepare many polymer/graphite composites with the

matrix being high density polyethylene (HDPE),¹⁰ polypropylene (PP),¹¹ ethylene vinyl acetate (EVA),¹² poly(ethylene terephthalate) (PET),¹³ and poly(ethylene-2,6-naphthalate) (PEN).¹⁴

PEI is an amorphous engineering plastic with the exceptional mechanical and thermal properties. It is widely used in the aerospace, transportation and microelectronics industries. A few of studies were carried out on the PEI/graphite based composites. In particular, Xian and Zhang¹⁵ studied the wear properties of PEI/graphite flake composites and found that the incorporation of graphite flakes improved the tribological properties at wide range of temperatures. Li et al.¹⁶ prepared the PEI/graphene nanoplatelet (GNP) composites by solution processing. An increase of the loss tangent, electrical conductivity and dielectric constant with the addition of GNP was shown. Wu et al.^{17–20} prepared PEI containing GNP of various sizes using different processing methods. The thermal conductivity of composites prepared by twin-screw extrusion increased with GNP particle size.¹⁷ These composites also exhibited low thermal expansion coefficients.¹⁸ PEI/GNP composites were also prepared by compression molding of GNP-precoated PEI powder in acetone. The electrical percolation threshold of these composites was found to be 2 wt % in comparison with

Table I. Properties of Graphites

Grade	Particle size	Carbon	Density	pH range
	89.5%, >44 μm	99%	2.2 g/cc	-
TC300	73%, >75 μm			
	40%, >150 μm			
3772	80%, >300 μm	99%	2.3 g/cc	5-10

10 wt % for the composites prepared by melt processing using twin-screw extruder. PEI and GNP powders were also ball milled and compression molded. In addition, GNP and PEI powders were compounded in a twin-screw extruder and subsequently subjected to ball milling with GNP powder. The electrical percolation threshold of ball milled composites was lower than that of the ball milled and extruded composites.¹⁹ They also carried out injection molding of PEI/GNP composites prepared by melt extrusion and found that their electrical resistivity, strength and modulus were higher than those of compression molded composites.²⁰

Over the two decades, an ultrasonically assisted extrusion was developed for processing plastics and rubbers.²¹ Extensive studies were also carried out in manufacturing polymer nanocomposites. It was reported that ultrasonic treatment improved dispersion of silica in EPDM,²² CNT in polyetherimide (PEI),²³ and CNF in PEI²⁴ and facilitated exfoliation of nanoclay in the polymer matrix in PP.²⁵

In this study, three different graphites, namely, natural graphite (UG), modified graphite (MG), and expanded graphite (EG), were incorporated into PEI to manufacture PEI/graphite composites by means of recently developed ultrasonic twin-screw extruder.²⁶ The rheological, mechanical, and electrical properties of the composites are investigated along with their morphology. The effect of ultrasound on dispersion and exfoliation of various graphites in PEI matrix was elucidated. It should be noted this is the first study where extensive comparison of various properties of PEI composites containing different graphites, prepared by ultrasonically assisted twin-screw extrusion, was carried out.

EXPERIMENTAL

Materials

Polyetherimide (PEI) in pellet form was supplied by SABIC (Pittsfield, MA) under trade-name ULTEM 1000. The UG (grade TC300) and expandable graphite (grade 3772) were both supplied by Asbury Carbons (Asbury, NJ). The properties of these two graphites are shown in Table I.

Preparation of Graphite

The preparation of MG was based on a method described in Ref. 27. By using this method, 30 g UG powder and 5 g sodium nitrate were mixed in 100 mL sulfuric acid. Ice bath was used to control temperature. Then, 25 g potassium permanganate and 5 g sodium nitrate was added slowly and kept for half an hour at a temperature below 20°C. Then the temperature was increased to 35°C and maintained for 1 h. After that 300 mL

water was added to dilute the solution. The mixture was filtered and washed by water to the pH value of 6. The graphite was then dried for 24 hours in an air ventilated oven at 80°C to obtain MG before expansion. The prepared powder was expanded in a muffle furnace (Barnstead Thermolyne 1300, Waltham, MA) for 10 s at temperature of 600°C to obtain MG. The EG was prepared by expanding the expandable graphite in a microwave oven (Panasonic AP104A, Newark, NJ) for 30 s.

Preparation of Composites

The melt processing was carried out using a co-rotating twin-screw micro-extruder (Prism USALAB 16, Thermo Electron Co., UK) modified by installing an ultrasonic unit (Branson Ultrasonics Corp., CT) close to the exit of the extruder, as shown in Figure 1(a). The ultrasonic unit consists of a converter, booster and water cooled titanium horn. The ultrasonic waves at a frequency of 40 kHz were delivered to the melt using power supply connected to a converter. The ultrasonic horn with a cross section area of $28 \times 28 \text{ mm}^2$ was in the direct contact with the polymer melt and provided the longitudinal vibrations in the direction perpendicular to the flow direction. The gap between the horn and screws was 2.5 mm with volume of an ultrasonic treatment zone of 1.9 cm^3 . Two pressure transducers (TPT412-5M-6, Dynisco Instruments, Sharon, MA) were mounted before and after the ultrasonic unit and one pressure transducer (PT460E-5M-6, Dynisco Instruments, Sharon, MA) was mounted in the die to record the pressure during processing. The imposition of ultrasonic waves on the polymer melt was digitally controlled by the ultrasonic power supply. An ultrasonic amplitude of 10 μm was applied to the polymer melt to study its effect on the dispersion of various graphites in a PEI melt. The diameter of the screws is 16 mm and L/D is 25. The screw configuration used is shown in Figure 1(b). There are three kneading block regions; KN1, KN2, and KN3. KN1 region contains nine discs with a staggering angle of 60° for the first five discs and 90° for the last four discs. KN2 region contains five discs with a staggering angle of 90°. KN3 region contains 8 discs with a staggering angle of 90° for the first four discs and -30° for the last four discs. PEI pellets were pre-dried in an oven at 65°C for 24 h before extrusion. These pellets were premixed with graphites at the required concentration and fed into the extruder by a feeder (K-Tron Soder, USA). The

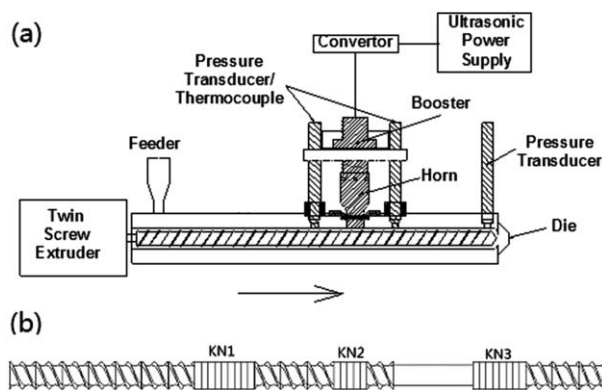


Figure 1. The schematic of ultrasonic twin-screw extruder (a) and the screw configuration (b).

temperature from the feeding zone to the die was 280°C, 350°C, 360°C, 360°C, and 360°C. The rotational speed used was 200 rpm, the flow rate was 1 lb/h.

Rheological Measurements

The rheological properties of the composites were studied using an Advanced Rheometric Expansion System (Model ARES LS, TA Instruments). The disc sample with a diameter of 25 mm and a thickness of 2.2 mm was used. It was prepared by compression molding using a compression molding press (CARVER 4122, Wabash, IN) at a pressure of 48.3 MPa and a temperature of 325°C. The disc sample was placed in a 25 mm parallel plate. A 1 mm gap was set by squeezing out the extra materials. This material was removed before the frequency sweep. Complex viscosity, tangent delta and storage and loss moduli were measured in the dynamic mode in a frequency range from 0.5 to 100 rad/s at 320°C in the linear viscoelastic region.

Electrical Resistivity

The composites with volume resistivity higher than $10^7 \Omega\text{-cm}$ were measured in accordance with ASTM D257 method using a Keithley electrometer (Model 6517A, Keithley Instruments, Cleveland, OH) equipped with a 8009 test fixture. An alternating polarity resistance test method with a voltage of $\pm 10 \text{ V}$ was used to eliminate the effect of background current. The composites with volume resistivity less than $10^7 \Omega\text{-cm}$ were measured using a Keithley Ohmmeter (Model 580, Cleveland, OH) based on the ASTM 4996. The discs with a diameter of 90 mm and a thickness of 1 mm for the electrical resistivity measurement were made using the same compression molding press at a pressure of 48.3 MPa and a temperature of 350°C.

XRD Characterization

XRD data were collected from three kinds of graphite powder in an X-ray diffractometer (Bruker AXS D8) using Cu K α radiation with a wavelength of 0.154 nm obtained at 40 kV and 40 mA. The scanning range was from 5° to 45° within a scanning time of 60 s.

Mechanical Properties

The tensile test was carried out according to the ASTM D638 using an Inston testing machine (Model 5567, Instron Corp., Canton, MA) with a 10 kN load cell at 25°C. The cross-head speed used was 5 mm/min. No extensometer was employed. The tensile test samples were prepared according to ASTM D638 using a minijet injection machine (DSM research micro-injection molding machine, Netherlands) at an injection pressure of 40 MPa and a melt temperature of 370°C and a mold temperature of 130°C.

Morphological Study

The morphological studies of all the graphites were carried out using a scanning electron microscope (HRSEM, Model JEOL JSM-7401F, Tokyo, Japan). The dispersion of all graphites in the PEI matrix was studied using an optical transmission microscope (Model Laborlux 12 POL S, Leitz Ltd., Midland, Ontario). The thin films of a thickness around 20 μm were cut using a microtome (Model 820, Reicher-Jung GmbH, Nussloch, Germany) from an injection molded dumbbell sample. The

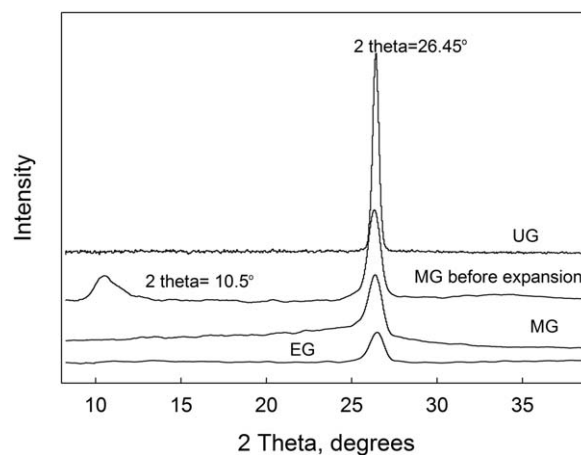


Figure 2. XRD spectra of UG, MG before expansion, MG and EG.

images were captured by a camera and then analyzed using the software ImageJ.

RESULTS AND DISCUSSION

Characteristics of Three Graphites

Figure 2 shows the XRD patterns of all the graphites used in this study. UG shows the distinguishable (002) peak at 26.45°, which is a typical peak of graphite with an interplanar distance of 0.336 nm. However, MG before expansion shows a new additional (001) peak at 10.5° with an interplanar distance of 0.841 nm. The distance change is due to the presence of oxygen functional groups generated by the modification and other defects in the structure.²⁸ Unlike the general graphene oxide,²⁹ the MG before expansion still has a strong (002) peak. It means the oxidation of graphite is quite limited. After expansion, MG only shows (002) peak, indicating that, similar to EG, the original crystal structure of graphite still exists. From the SEM images in Figure 3, it is seen that the surface of UG is very dense [Figure 3(a)]. However, for MG before expansion, a fraction of layers are delaminated to some extent [Figure 3(b)]. The further expansion created a kind of “Lasagna” structure, in which many delaminated sub-layers in scale of microns are connected with each sub-layer still containing hundreds of graphene layers [Figure 3(c)]. The latter layers have the same crystalline structure as the original graphite. This is the reason for an appearance of the strong (002) peak for MG in Figure 2. Compared to the UG and MG, EG exhibits a much more exfoliated structure [Figure 3(d)] with the stack of nanosheets of the thickness varying from 100 to 400 nm.³⁰ Each nanosheet still contains many layers of graphene providing a strong (002) peak in the XRD diffraction.

Process Characteristics

Table II lists the ultrasonic power consumption applied to the polymer melt in the extruder at different graphite concentrations. Some portion of this power is dissipated as heat leading to the temperature rise in the material, other portion is applied to disperse graphite in the polymer melt. From Table II, it is observed that for pure PEI, the power consumption at an amplitude of 10 μm is lower than that for PEI/graphite composites. It means that an extra power is exerted to the dispersion

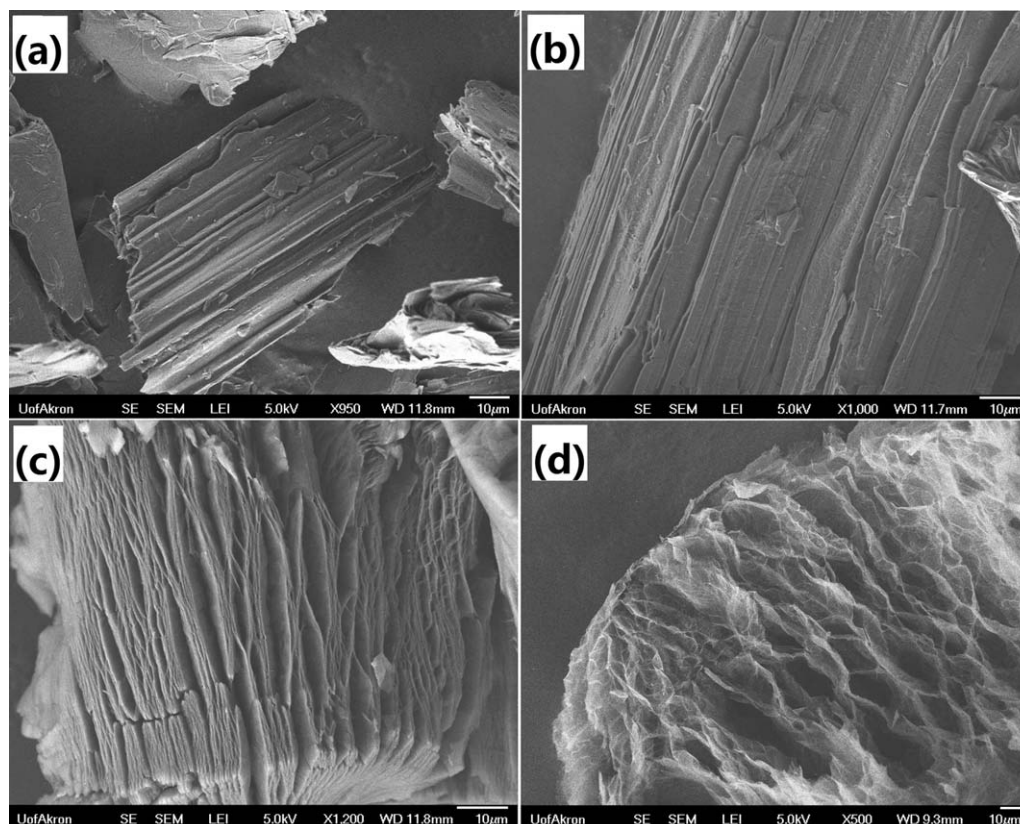


Figure 3. SEM images of UG (a), MG before expansion (b), MG (c), and EG (d).

of graphite. For PEI/UG and PEI/EG composites, the power consumption in the composite of a 10 wt % graphite is the highest. But for PEI/MG, the highest power consumption occurs at 5% concentration. It means more energy was transmitted to the polymer melt at that content.¹⁷ Table III shows the torque given as percentage of the maximum torque of the extruder. It is observed that the torque does not change significantly with the concentration of different graphites. The latter is due to the high shear rate used in the processing, because at high shear rates as shown below, the difference of viscosity at all concentrations is insignificant. Accordingly, it is expected little changes in the torque with an increase of graphite content. However, when the ultrasound at an amplitude of 10 μm is applied to the system, the torque is decreased. This is due to the prevailing thixotropic effect on viscosity reduction, if any, induced by the ultrasonic wave over viscosity increase in the composites due to improved dispersion. However, there are still

Table II. Ultrasonic Power Consumption of PEI/Graphite Composites with Ultrasonic Treatment at an Amplitude of 10 μm

Content	PEI/UG, W	PEI/MG, W	PEI/EG, W
0	40.7 \pm 4.8	40.7 \pm 4.8	40.7 \pm 4.8
2.5%	56.8 \pm 6.0	66.3 \pm 5.8	76.9 \pm 8.2
5%	51.4 \pm 5.5	75.6 \pm 7.3	77.9 \pm 8.2
7.5%	52.3 \pm 5.3	63.9 \pm 7.6	74.9 \pm 8.1
10%	72.9 \pm 7.4	66.9 \pm 7.7	101.9 \pm 7.6

little differences in the torque at different graphite contents. Also, it should be noted that during extrusion the pressures indicated by three pressure transducers were too low to be reported.

Rheological Properties

Figure 4 shows the complex viscosity (a), $\tan \delta$ (b), storage (c), and loss (d) moduli as a function of frequency for the untreated and ultrasonically treated PEI, PEI/UG and PEI/MG at a 5 wt % graphite loading. It can be seen that all these properties of the PEI/UG, with or without ultrasonic treatment, are not significantly different compared to those of the pure PEI. The latter is attributed to the large particle size of UG and bad dispersion of the original graphite in the matrix, as shown later in the morphology section. The results are similar to that reported by King et al.,³¹ which showed that the rheological properties changed little at graphite concentrations below 30 wt %. However, after modification, the complex viscosity of PEI/MG composites [Figure 4(a)] is noticeably increased, which is due to the increased surface area of MG particles as seen from Figure 3(c). After the ultrasonic treatment at an amplitude of 10 μm , the PEI/MG composite indicates a significantly increased complex viscosity especially in the lower frequency region. This effect can be explained in the way that the acoustic cavitation broke the “Lasagna” structure leading to a further increase of the surface area of the graphite. The latter also helps to provide a more uniform dispersion of MG in the PEI matrix, as shown for other type of fillers in various polymers.^{15–19} This statement is further substantiated by a decrease of $\tan \delta$ [Figure 4(b)] and

Table III. Torque During Extrusion of PEI/Graphite Composites without and with Ultrasonic Treatment

Content	Torque of PEI/UG, %		Torque of PEI/MG, %		Torque of PEI/EG, %	
	Untreated	10 μm Ultrasound	Untreated	10 μm Ultrasound	Untreated	10 μm Ultrasound
0	67.3 \pm 3.9	58.8 \pm 6.0	67.3 \pm 3.9	58.8 \pm 6.0	67.3 \pm 3.9	58.8 \pm 6.0
2.5%	70.1 \pm 5.1	58.2 \pm 5.6	66.5 \pm 3.4	54.3 \pm 2.1	68.2 \pm 3.9	53.4 \pm 3.6
5%	71.2 \pm 3.7	55.6 \pm 7.4	67.9 \pm 5.6	56.4 \pm 3.9	66.5 \pm 3.5	55.6 \pm 4.4
7.5%	68.5 \pm 4.5	55.3 \pm 3.4	69.2 \pm 4.3	56.7 \pm 2.6	70.6 \pm 3.5	56.4 \pm 3.6
10%	71.6 \pm 4.8	55.9 \pm 3.7	70.4 \pm 3.4	59.1 \pm 2.5	68.7 \pm 4.2	53.6 \pm 3.4

an increase of the storage [Figure 4(c)] and loss moduli [Figure 4(d)] after ultrasonic treatment of this composite. It can be seen that all these differences are much higher in the low frequency region than in the high frequency region.

Quite different rheological behavior is observed for the PEI/EG composite of various concentrations (Figure 5). Their complex viscosity is clearly increased with increasing graphite concentration. In particular, at a 10 wt % concentration, its viscosity in the low frequency region is almost one order of magnitude higher than that of the pure PEI. Furthermore, the ultrasonically treated composites consistently show a higher viscosity than the untreated ones [Figure 5(a)]. The latter is resulted from a better exfoliation of the layered structure of EG and its

better dispersion of EG in the matrix. It can be seen in Figure 5(a) in the low frequency region, there is a Newtonian plateau for pure PEI, but for PEI/EG composites with graphite concentration of 2.5 wt % or more, this plateau began to disappear. A strong shear thinning behavior can be seen at high concentration composite.

This rheological behavior was also seen in the previous study on PC/EG and PS/EG composites with an increasing EG concentration.³²

The effect of ultrasound is also observed from $\tan \delta$, the storage and loss moduli of PEI/EG composites in Figure 5(b–d). After ultrasonic treatment, the storage and loss moduli are increased with increasing concentration. Both the effect of ultrasound and

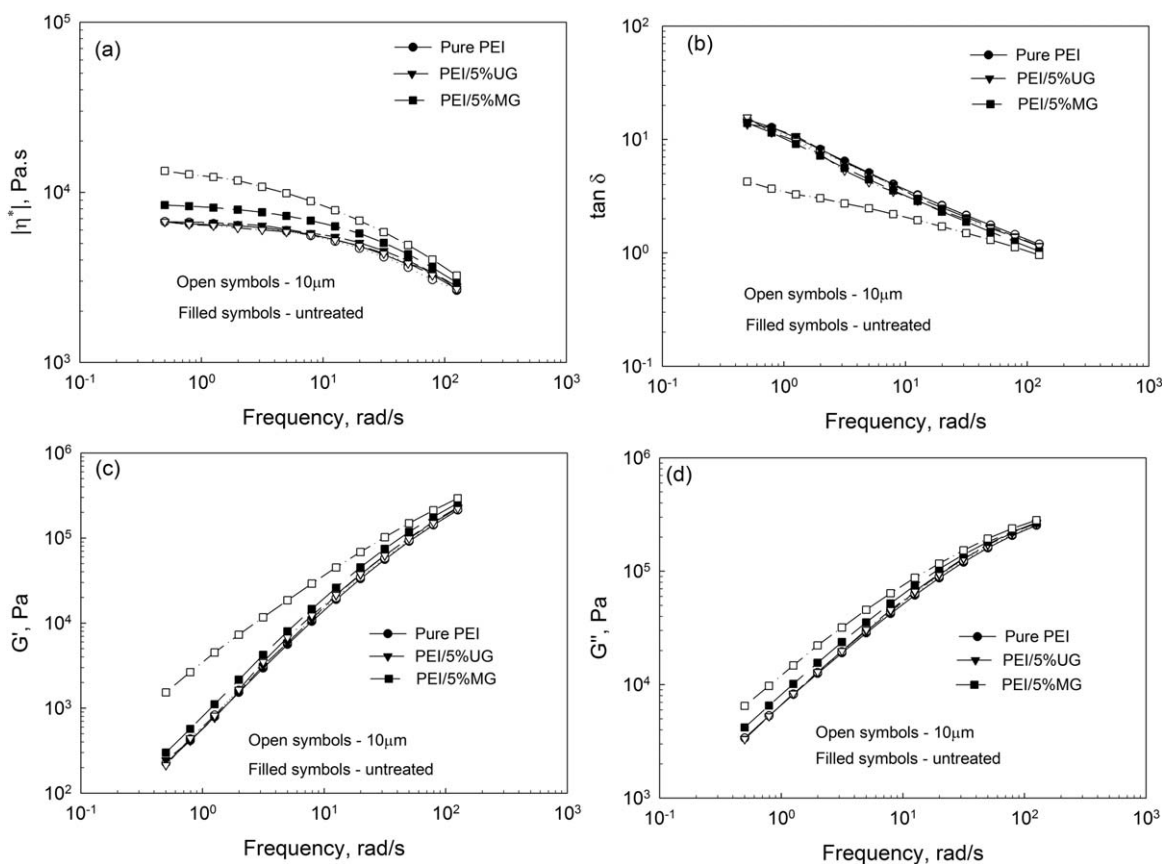


Figure 4. Complex viscosity (a), $\tan \delta$ (b), storage (c), and loss moduli (d) as a function of frequency for untreated and ultrasonically treated pure PEI, PEI/UG and PEI/MG at 5 wt % graphite loading.

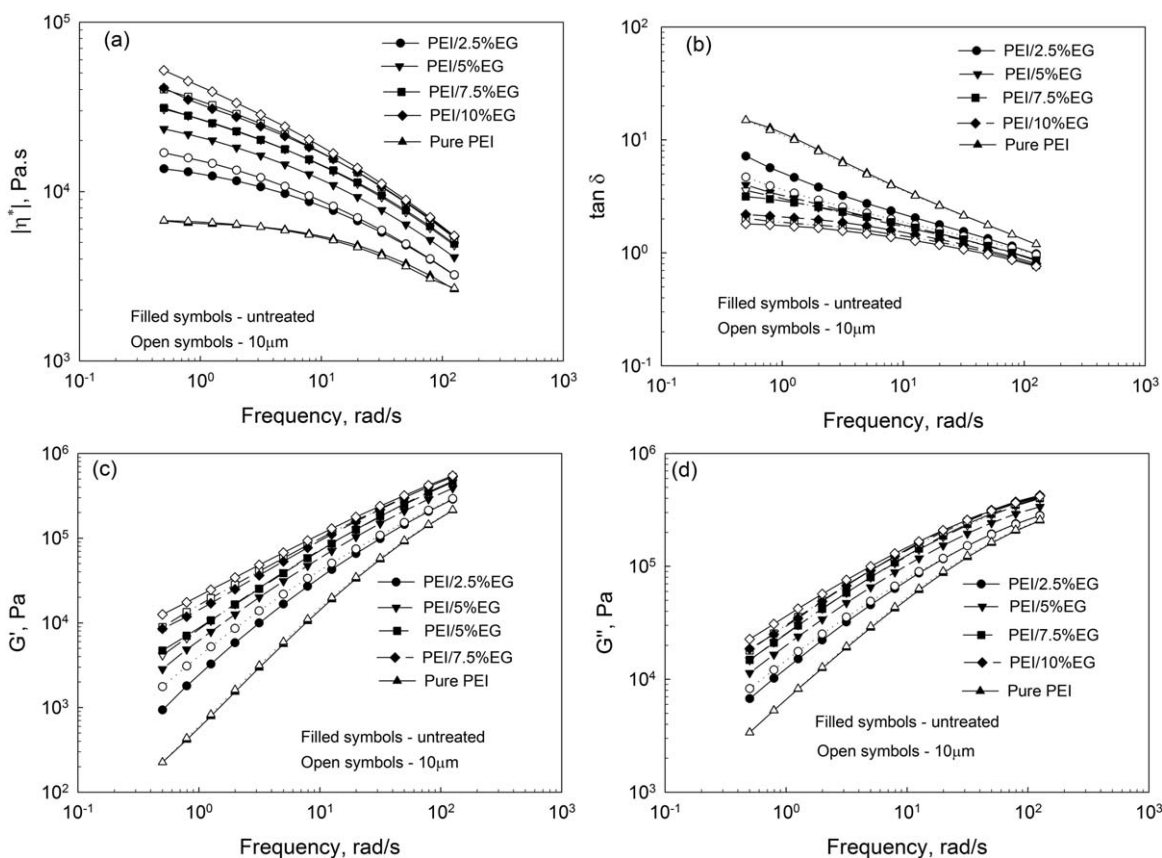


Figure 5. Complex viscosity (a), $\tan \delta$ (b), storage (c), and loss (d) moduli as a function of frequency for untreated and ultrasonically treated PEI/EG at different graphite loadings.

graphite concentration is more pronounced in the low frequency region. With ultrasonic treatment at an amplitude of 10 μm , the storage modulus at low frequency is increased by almost two orders of the magnitude at 10 wt % compared to the pure PEI. At this high concentration, the storage modulus shows a weaker dependence on the frequency. This indicates a gradual build up of some kind of fillers and polymer-filler network structure restricting the motion of the PEI chains.

The $\tan \delta$ is seen to decrease with graphite concentration and ultrasonic treatment, especially in the low frequency region, that is because of more increase of the storage modulus than the loss modulus occurred. The decreased value of $\tan \delta$ of ultrasonically treated composites also indicates a better dispersion of EG in the polymer and its better interaction with the polymer chains. At high concentration, the slope of $\tan \delta$ -frequency curve is reduced, which means that the network structure greatly affects the relaxation behavior of the PEI chains.

The complex viscosity of PEI/UG, PEI/MG and PEI/EG at a 0.5 rad/s frequency as a function of graphite concentration is presented in Figure 6. The viscosity increases with an increase of graphite concentration and ultrasonic treatment. However, no percolation was observed in this concentration range. Apparently, the percolation is in higher concentration region. In fact, the rheological percolation threshold for CNT and CNF in PEI is, respectively, reported to be 1–2 wt %²³ and 15–20 wt %²⁴

with ultrasonic treatment. For PEI/UG composites little increase in the viscosity is observed with an increase of the graphite concentration, because the graphite particles are very large and agglomerated at high concentration. However, for the PEI/MG composites, the complex viscosity first increases with MG concentration till 5 wt % then decreases with concentration. There are two possible reasons for this trend. First, the composites at high concentration may agglomerate to bigger sizes. Second, the

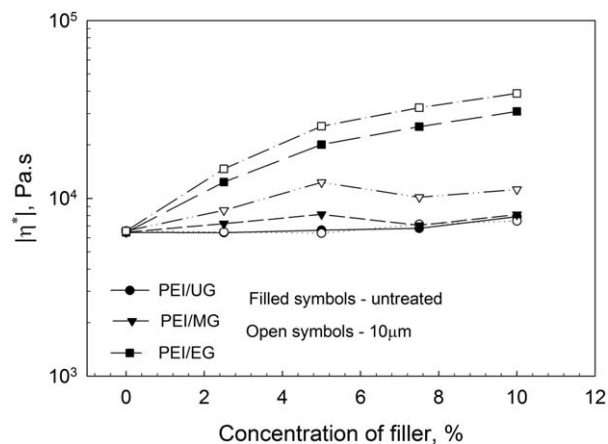


Figure 6. Complex viscosity of PEI/UG, PEI/MG, and PEI/EG as a function of graphite concentration at a frequency of 0.5 rad/s.

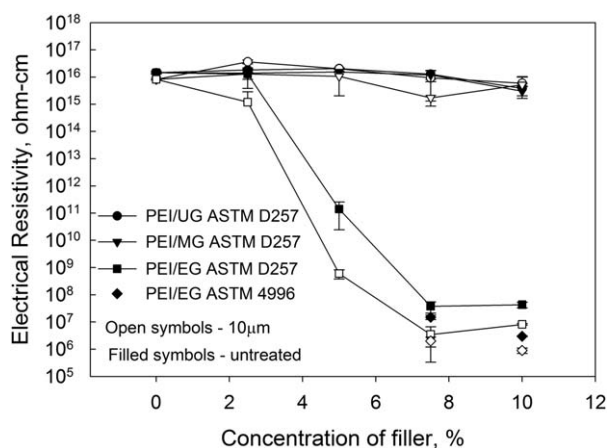


Figure 7. Volume resistivity of PEI/UG, PEI/MG and PEI/EG composites without and with ultrasonic treatment as a function of graphite concentration.

modification of UG using acid may induce the degradation of PEI especially at higher concentration of graphite due to the presence of acid residue. However, the ultrasonic treatment at an amplitude of $10\ \mu\text{m}$ shows higher viscosity at any concentration of PEI/MG composites.

Electrical Properties

Figure 7 shows the volume resistivity of PEI/graphite composites as a function of the graphite concentration based on two ASTM methods. It is suggested (suspected) that ASTM D257 can be used to measure the resistivity above and below $10^7\ \Omega\text{-cm}$. However, comparison of the two methods indicates that the resistivity measured by ASTM 4996 at around $10^7\ \Omega\text{-cm}$ provides different values. In fact, the resistivity of PEI/EG composites measured using ASTM D257 is about the same at 7.5 wt % and 10 wt % concentration while the resistivity measured by ASTM 4996 method shows lower values and decreases with EG content. Therefore, it is concluded that the volume resistivity measurement from ASTM D257 and ASTM 4996 methods is suitable for value of above and below $10^7\ \Omega\text{-cm}$, respectively. For PEI/UG and PEI/MG composites, the volume resistivity does not change with graphite concentration and ultrasonic treatment. The latter is attributed to large size of the graphite particles that are unable to build a conducting network, even at a 10 wt % concentration of UG and MG. These composites are still electrical insulators. A previous study using the same UG³³ achieved the electrical percolation at a concentration above 20 wt %. That is why percolation is not seen in the present study. However, the resistivity of PEI/EG composites show a sharp reduction at 5 wt % concentration for both without and with ultrasonic treatment at an amplitude of $10\ \mu\text{m}$. The electrical percolation threshold occurs between 2.5 and 5 wt %. When the graphite content exceeds the percolation threshold, a graphite network is built up to make a conductive path, such that the composite starts to behave like a conductor. This electrical percolation threshold is similar to the value at about 5 wt % obtained for LLDPE composites using the same EG.³⁴ In addition, it is seen from Figure 7 that after the ultrasonic treatment

at an amplitude of $10\ \mu\text{m}$, the volume resistivity is lower than that without treatment reducing the percolation threshold. At a 5 wt % concentration of EG, the resistivity is almost three orders of magnitude lower when an ultrasonic amplitude of $10\ \mu\text{m}$ is applied. This indicates that ultrasound is beneficial for good dispersion of EG assisting the graphite to establish a conductive network at a lower concentration.

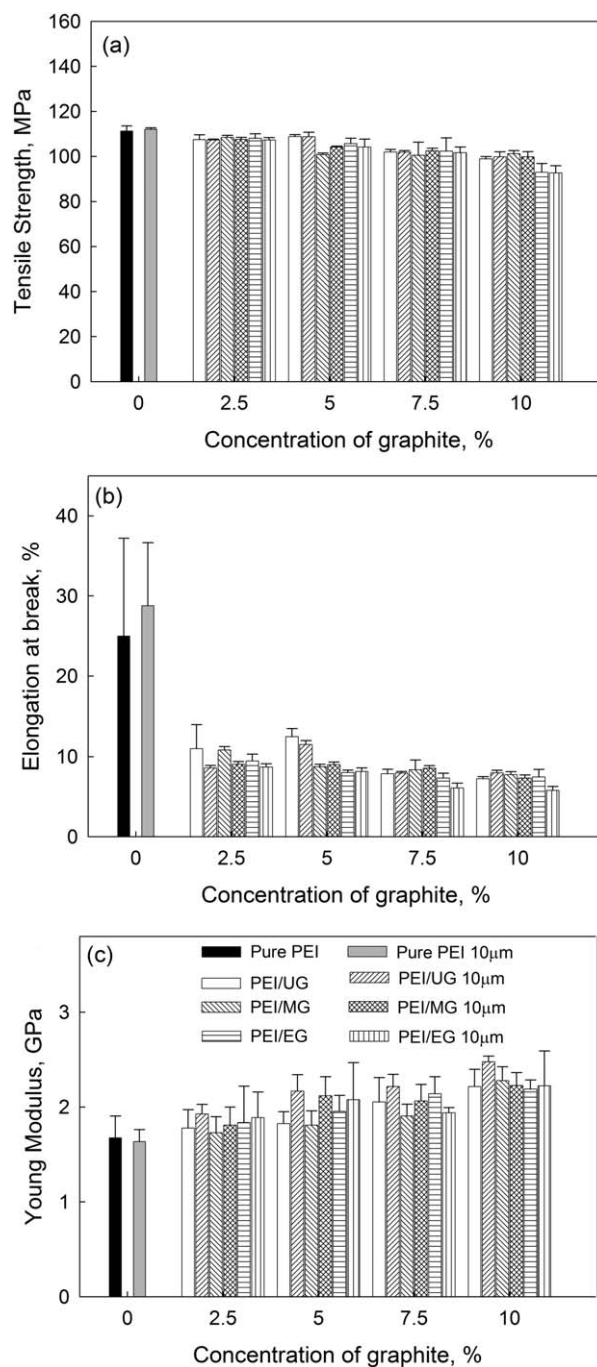


Figure 8. Tensile strength (a), elongation at break (b), and Young's modulus (c) of PEI/UG, PEI/MG and PEI/EG composites as a function of the graphite concentration without and with ultrasonic treatment at an amplitude of $10\ \mu\text{m}$.

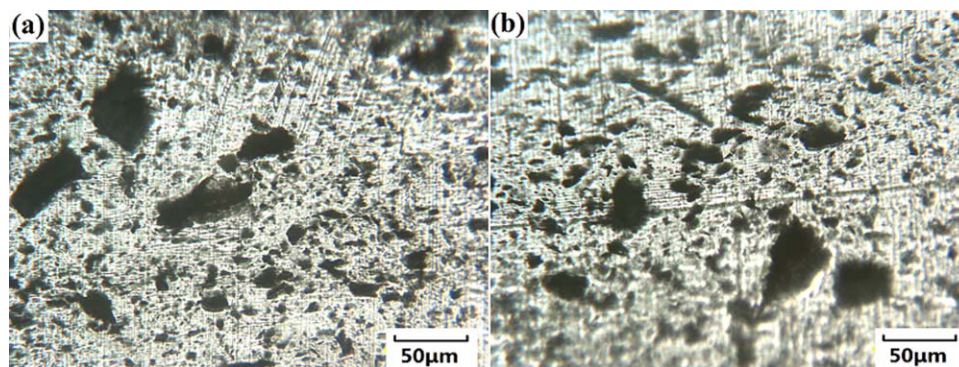


Figure 9. Optical micrographs of PEI/5 wt %UG composites without ultrasonic treatment (a) and with ultrasonic treatment at an amplitude of 10 μm (b). [Color figure can be viewed in the online issue, which is available at wileyonlinelibrary.com.]

Mechanical Properties

The tensile strength is defined as the highest stress developed during tensile testing. Figure 8 compares the tensile strength of untreated and ultrasonically treated PEI/UG, PEI/MG and PEI/EG composites of various the concentrations of graphite. It is clear that all the composites show a tendency to decrease the tensile strength with an increase of the concentration of graphite. This observation is different from the tensile stress behavior of PEI/CNT²³ and PEI/CNF²⁴ composites. The tensile strength of PEI/CNT composites showed an increase with concentration and PEI/CNF at a concentration lower than 15 wt % showed the tensile strength comparable to that of the pure PEI and then decreases with concentration. At a 10 wt % concentration, the tensile strength of PEI/EG composites shows the strength of

93.0 MPa, which is 16.4% lower than that of the pure PEI having a tensile strength of 111.2 MPa. Such a behavior of PEI/EG is different from the behavior of PPS/EG composites and PEI/GNP composites. For PPS/EG composites, the flexural strength firstly decreased and then increased with EG concentration,³⁵ while for PEI/GNP composites the strength increased by about 10% at concentration of 5 wt % compared to pure PEI.²⁰ Also, as seen from Figure 8(a), the ultrasonic treatment does not show any effect on the tensile strength of the composites. The elongation at break of different PEI/graphite composites is presented in Figure 8(b). The elongation at break decreases drastically at 2.5 wt % concentration for all the composites, because the graphite filler acts as a stress concentrator within PEI. With further increase of concentration, it decreases gradually. The

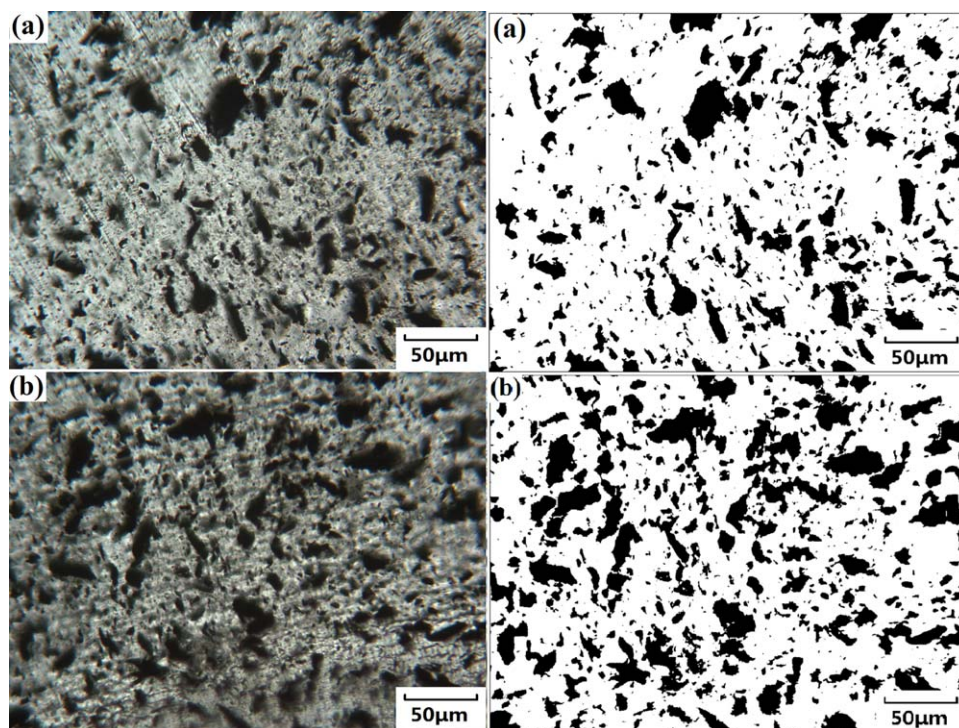


Figure 10. Optical micrographs of PEI/5 wt % MG composites without ultrasonic treatment (a) and with ultrasonic treatment at an amplitude of 10 μm (b). Micrographs on the right-hand side are obtained by using the ImageJ software. [Color figure can be viewed in the online issue, which is available at wileyonlinelibrary.com.]

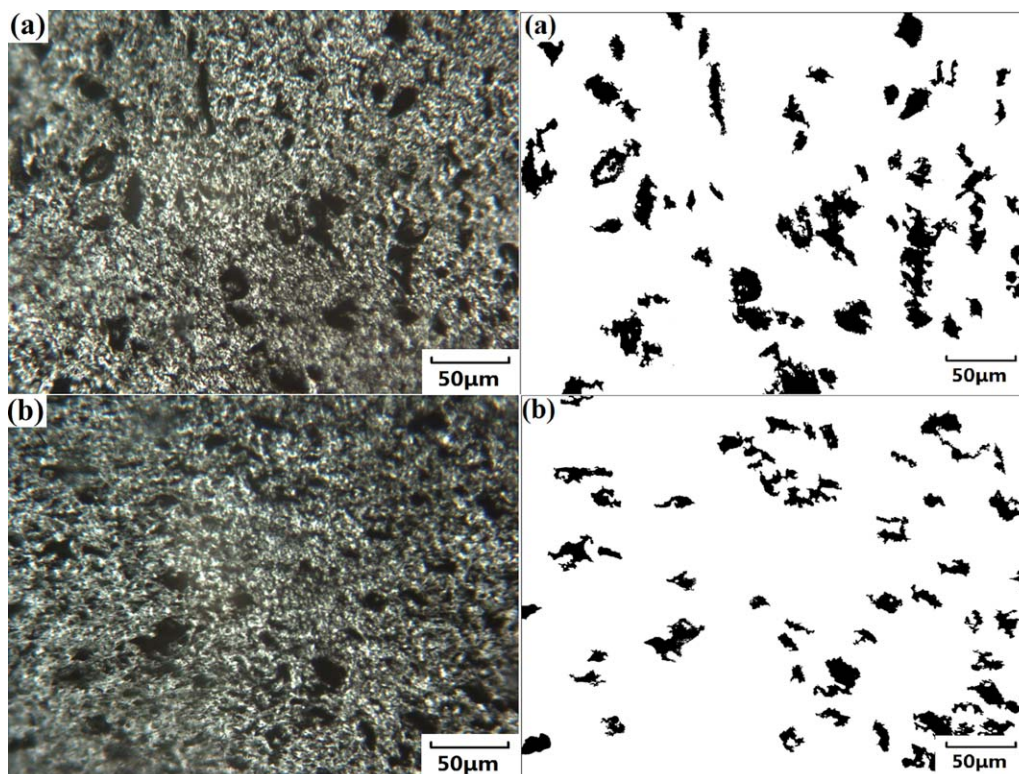


Figure 11. Optical micrographs of PEI/5 wt % EG composites without ultrasonic treatment (a) and with ultrasonic treatment at an amplitude of $10\ \mu\text{m}$ (b). Micrographs on the right-hand side obtained by the ImageJ software show the agglomerate of larger than $100\ \mu\text{m}^2$. [Color figure can be viewed in the online issue, which is available at wileyonlinelibrary.com.]

ultrasonic treatment does not bring any difference in such a behavior. The Young's modulus of different composites is increased with graphite concentration, as shown in Figure 8(c). But this increase of the modulus is not as high as in case of addition of CNT²³ and CNF²⁴ to PEI. Unlike the different rheological properties of untreated and ultrasonically treated composites, there is no significant improvement in the Young's modulus of composites with ultrasonic treatment at an amplitude of $10\ \mu\text{m}$.

Morphological Analysis

Sizes of all the graphites used in the present study are on the scale above micrometers. This makes optical microscopy a good tool for characterizing the structure and dispersion of graphite in PEI. Figure 9 shows the optical micrographs of PP/5%UG without treatment (a) and with ultrasonic treatment at an amplitude of $10\ \mu\text{m}$ (b). Some large graphite particles or agglomerates as well as many small particles are seen. Large particles are of similar sizes as those of the UG particles. Small particles are mostly generated through the breakage of the large particles. It demonstrates that the ultrasonic treatment brings little change to the final structure and dispersion of UG particles. In Figure 10, the size of MG particle is smaller than the size of UG particle shown in Figure 9 in both cases without and with ultrasonic treatment. Evidently the loose "Lasagna" structure is easily broken during the extrusion. With the assistance of ImageJ software, the graphites and PEI phase are clearly seen as shown on the right of Figure 10. The dark area ratio calculated

by ImageJ for PEI/5%MG composites without and with ultrasonic treatment is 20.1% and 29.2%, respectively. It is clear that the layered MG particles are partially exfoliated by the ultrasound and the area occupied by the graphite is increased. This indicates a favorable effect of ultrasound on breakup of the MG layered structure. For PEI/EG composites, Figure 11 shows much darker background than that in PEI/UG and PEI/MG composites. The latter means better dispersion of EG particle in the PEI matrix. This reduces the light transmission through the sample. The agglomerates with area larger than $100\ \mu\text{m}^2$ are selected with the help of ImageJ software and shown on the right of Figure 11. It is obvious that the number of large agglomerates is decreased with ultrasonic treatment at an amplitude of $10\ \mu\text{m}$.

CONCLUSION

An ultrasound assisted twin-screw extruder was employed to investigate the effect of ultrasonic treatment on exfoliation and dispersion of various graphite particles in the PEI matrix. The ultrasonic treatment shows little effect on exfoliation of the untreated graphite (UG) and its dispersion, due to its large size and dense structure. Their rheological, electrical and mechanical properties do not change much with ultrasonic treatment. However, after modification, graphite exhibits a "Lasagna" structure and the ultrasonic treatment promotes separation of layers in MG to create more surface area. This leads to an increase of the viscosity, storage and loss moduli and a decrease in $\tan\ \delta$. But the electrical and mechanical properties are not significantly

affected even at the graphite concentration of 10 wt %. For the expanded graphite, ultrasonic treatment causes a significant increase of the complex viscosity, storage and loss moduli and a reduction of $\tan \delta$, an increase of the electrical conductivity and a decrease of the percolation threshold, due to the creation of more surface area and better dispersion. The morphological study using optical microscopy supported all these findings.

ACKNOWLEDGMENTS

Financial support of this work by NSF grant no. CMMI-1131342 is greatly appreciated. The authors also wish to thank Asbury Carbons and SABIC for providing carbon materials and PEI resins.

REFERENCES

1. Kroto, H. W.; Heath, J. R.; O'Brien, S. C.; Curl, R. F.; Smalley, R. E. *Nature* **1985**, *318*, 162.
2. Iijima, S. *Nature* **1991**, *354*, 56.
3. Potts, J. R.; Murali, S.; Zhu, Y.; Zhao, X.; Ruoff, R. S. *Macromolecules* **2011**, *44*, 6488.
4. Sengupta, R.; Bhattacharya, M.; Bandyopadhyay, S.; Bhowmick, A. K. *Prog. Polym. Sci.* **2011**, *36*, 638.
5. Jacob George, J.; Bandyopadhyay, A.; Bhowmick, A. K. *J. Appl. Polym. Sci.* **2008**, *108*, 1603.
6. Boehm, H. P.; Setton, R.; Stumpp, E. *Pure Appl. Chem.* **1994**, *66*, 1893.
7. Stevens, R. E.; Ross, S.; Wesson, S. P. *Carbon* **1973**, *11*, 525.
8. Kim, H.; Miura, Y.; Macosko, C. W. *Chem. Mater.* **2010**, *22*, 3441.
9. Paul, D. R.; Robeson, L. M. *Polymer* **2008**, *49*, 3187.
10. Li, Y.-C.; Chen, G.-H. *Polym. Eng. Sci.* **2007**, *47*, 882.
11. Qu, S.; Wong, S.-C. *Compos. Sci. Technol.* **2007**, *67*, 231.
12. Ghose, S.; Watson, K. A.; Working, D. C.; Connell, J. W.; Smith, J. G., Jr.; Sun, Y. P. *Compos. Sci. Technol.* **2008**, *68*, 1843.
13. Zhang, M.; Li, D.-J.; Wu, D.-F.; Yan, C.-H.; Lu, P.; Qiu, G.-M. *J. Appl. Polym. Sci.* **2008**, *108*, 1482.
14. Kim, H.; Macosko, C. W. *Macromolecules* **2008**, *41*, 3317.
15. Xian, G. J.; Zhang, Z. *Wear* **2005**, *258*, 783.
16. Li, B.; Olson, E.; Perugini, A.; Zhong, W.-H. *Polymer* **2011**, *52*, 5606.
17. Wu, H.; Drzal, L. T. *Polym. Compos.* **2013**, *34*, 2148.
18. Wu, H.; Drzal, L. T. *Mater. Chem. Phys.* **2014**, *146*, 26.
19. Wu, H.; Rook, B.; Drzal, L. T. *Polym. Compos.* **2013**, *34*, 426.
20. Wu, H.; Drzal, L. T. *J. Appl. Polym. Sci.* **2013**, *130*, 4081.
21. Isayev, A. I.; Wong, C. M.; Zeng, X. *Adv. Polym. Technol.* **1990**, *10*, 31.
22. Isayev, A. I.; Hong, C. K.; Kim, K. *J. Rubber Chem. Technol.* **2003**, *76*, 923.
23. Isayev, A. I.; Kumar, R.; Lewis, T. M. *Polymer* **2009**, *50*, 250.
24. Isayev, A. I.; Jung, C.; Gunes, K.; Kumar, R. *Int. Polym. Process.* **2008**, *4*, 395.
25. Lapshin, S.; Isayev, A. I. *J. Vinyl Addit. Technol.* **2006**, *12*, 78.
26. Isayev, A. I.; Liang, T.; Lewis, T. M. *Rubber Chem. Technol.* **2013**, *87*, 86.
27. Hummers, W. S.; Offeman, R. E. *J. Am. Chem. Soc.* **1958**, *80*, 1339.
28. Zhao, J.; Pei, S.; Ren, W.; Gao, L.; Cheng, H.-M. *ACS Nano* **2010**, *4*, 5245.
29. Ban, F. Y.; Majid, S. R.; Huang, N. M.; Lim, H. N. *Int. J. Electrochem. Sci.* **2012**, *7*, 4345.
30. Chen, G.-H.; Wu, D.-J.; Weng, W.-G.; Yan, W.-L., *J. Appl. Polym. Sci.* **2001**, *82*, 2506.
31. King, J. A.; Morrison, F. A.; Keith, J. M.; Miller, M. G.; Smith, R. C.; Cruz, M.; Neuhalfen, A. M.; Barton, R. L. *J. Appl. Polym. Sci.* **2006**, *101*, 2680.
32. Abdel-Goad, M.; Pötschke, P.; Zhou, D.; Mark, J. E.; Heinrich, G. *J. Macromol. Sci., Part A: Pure Appl. Chem.* **2007**, *44*, 591.
33. King, J. A.; Via, M. D.; Keith, J. M.; Morrison, F. A. *J. Compos. Mater.* **2009**, *43*, 3073.
34. Kim, S.; Seo, J.; Drzal, L. T. *Composites Part A* **2010**, *41*, 581.
35. Zhao, Y. F.; Xiao, M.; Wang, S. J.; Ge, X. C.; Meng, Y. Z. *Compos. Sci. Technol.* **2007**, *67*, 2528.